TEXTURE AND SURFACE CHEMISTRY OF ACTIVATED CARBONS OBTAINED FROM TYRE WASTES.

Beatriz Acevedo* , Carmen Barriocanal

[a] Instituto Nacional del Carbón, INCAR-CSIC, Apartado 73, 33080 Oviedo. Spain

*Corresponding author. Tel: +34 985 11 90 90; Fax:+34 985 29 76 62; e-mail address: beatriz.acevedo@incar.csic.es

ABSTRACT

Tyre wastes and their blends with coal and a bituminous waste material obtained from the benzol distillation column of the by-product section of a coking plant were employed as a precursor for the production of activated carbons (ACs). Pyrolysis up to 850 °C followed by physical activation with CO_2 yielded mesoporous carbons with different pore size distributions and surface areas depending on the degree of burn-off. ACs with surface areas of 475 and 390 m^2/g were obtained for the two tyre wastes. The inclusion of coal in the blend gave rise to surface areas of up to 1120 m^2/g due to an increase in the microporosity. The time needed to obtain the desired degree of burn-off depended on the reactivity of the char. The coal-containing materials required the longest amount of time. The surface chemistry of the samples was studied by Infrared spectroscopy (FTIR) and X-Ray photoelectron spectroscopy (XPS). The principal oxygenated groups found were quinones, lactones and carboxylic acids.

Keywords: Scrap tyres, reinforcing fibre, coal, activated carbons, surface chemistry.

1. Introduction

The preparation of activated carbons has been the subject of extensive research study for many years [1-13] due to the diversity of their applications. Mainly though, activated carbons have been used as adsorbents and catalysts [14-19].

Although it is the porous structure of activated carbons that will determine their performance, the presence of surface groups containing heteroatoms will confer upon them different chemical properties that will contribute to determining their final application.

Activated carbons can be produced from a range of carbonaceous materials including coal or biomass (coconut shell, wood, coir pitch, cellulosic waste orange peel, sawdust, rice-husk, etc.) [20-25]. Waste tyres represent another valuable source of activated carbons because of their high carbon content [26]. This would also provide a way of recovering waste tyres, the generation of which is constantly increasing, causing numerous economic and environmental problems. Tyre material recycling is normally carried out by means of a shredding procedure that yields granulated rubber as its product and steel and reinforcing fibre in the form of fluff as sub-products. Rubber crumbs are applied in sports surfaces and as an additive for asphalt, etc. but so far no real use has been found for the fluff.

The pyrolysis of tyre wastes yields three products: gas with a high calorific value, pyrolytic oil that can be used as fuel and as a source of benzene, toluene, xylene (BTX), and limonene and thirdly char that can be used as fuel, adsorbent or carbon black [27-32]. In order to obtain products with a high percentage of carbon and low ash content, co-pyrolysis with coal or bituminous wastes is a good option [26, 33, 34]. The co-processing of tyre crumbs with coal has also been studied as a way to improve coal liquefaction and hydro-pyrolysis [26, 33, 35, 36]. However until now little work has been carried out on the co-pyrolysis of tyre wastes (reinforcing fibre and tyre crumbs) with coal or with a bituminous waste [34].

The objective of the present study is to investigate the activation of chars obtained from two tyre wastes and their blends with coal and a bituminous residue that have different porous textures and surface chemistry characteristics.

2. Materials and Methods

2.1 Materials

Three components are obtained from the grinding of scrap tyres: tyre crumbs, reinforcing fibre and steel. In the present study tyre crumbs and reinforcing fibre were used to prepare tyre waste – derived activated carbons (ACs).

The wastes used as raw materials for the production of the ACs were: tyre crumbs (TC) and reinforcing fibres (RF) derived from the grinding of End-of-Life-Tyres (ELTs), 1:1 blends of TC and RF with a low rank coal, and 1:1 blends of RF with a bituminous waste material (BWM).

The chars were produced in a rotary oven (5ºC/min up to 850ºC with a soaking time of 30 minutes) and in a nitrogen atmosphere as explained in a previous paper [26]. Physical activation was also carried out in the rotary oven at 850ºC with a flow of 250 ml/min of CO_2 for various periods of time in order to obtain different degrees of burn-off expressed on an ash free basis (B.O.) throughout the manuscript.

The elemental analysis was carried out using a LECO CHN-2000 instrument for the C, H and N analysis, a LECO S-144 DR device for the sulphur analysis and a LECO VTF-900 instrument for direct oxygen determination.

2.2 Textural characterization

The textural properties of the ACs were studied from N_2 adsorption isotherms at 77 K on a Micromeritics ASAP 2420 apparatus. The software package provided with the equipment was used to determine the BET surface area (S_{BET}) and the total pore volume (V_t) at p/p_0=0.97. The micropore volume (V_{micro}) was determined by applying the Dubinin-Radushkevich (D-R) equation to the lower relative pressure zone of the isotherm. The mesopore volume (V_{meso}) was calculated by subtracting the micropore volume from the total pore volume (V_t). The Kelvin condensation theory was employed to examine the mesopore volume distribution [37]. The samples (approximately 0.25 g) were degasified under vacuum at 200 °C for 12 h prior to N_2 adsorption to eliminate any moisture and condensed volatiles.

The IUPAC pore size classification that assigns a size of 2-50 nm to mesopores and a size of <2 nm to micropores was employed.

2.3. Surface chemistry

Fourier transform infrared spectroscopy (FTIR) spectra were recorded on a Nicolet Magna-IR560 spectrometer equipped with a DTGS detector that operates at ambient temperature. Samples were prepared in the form of pellets using KBr as a matrix, in a ratio of 1 mg of sample to 600 mg of KBr. The pellets were dried at 120 °C for 24 h before analysis. The spectra were recorded from 4000 to 400 cm^{-1} by 128 interferograms at a resolution of 4 cm^{-1}.

X-Ray photoelectron spectroscopy (XPS) measurements were taken on a SPECS spectrometer equipped with a Phoibos 100 hemispherical analyzer. The X-ray radiation source was a monochromatic Al Ka (1486.74 eV) with a 100 W X-ray power and an anode voltage of 14.00 kV. The photo-excited electrons were analyzed in constant pass energy mode, using pass energy of 50 eV for the survey spectra and 10 eV for the high resolution core level spectra. CasaXPS software was employed for data processing. The compositions in atomic percentage (at. %) were determined from the survey spectra on the basis of the integrated peak areas of the main XPS peaks of the different elements (C(1s), N(1s), O(1s), S(2p) and Si(2p)) and their respective sensitivity factors.

3. Results and discussion

Examination of the activation curves provides very useful information for controling the activation process and determining the production cost. Physical activation depends on the reactivity of the char and the type of activating agent used. The activation curves obtained using CO_2 as activating agent are shown in Figure 1. These curves represent the time required to obtain a specific burn-off on an ash free basis. All the materials show a linear trend with the exception of RF where the slope changes at 65 wt% BO. These results indicate that activation proceeded in a gradual way independently of the development of

porosity [38]. The slope of the lines is a measure of the reactivity of the material. It can be seen that the material which needed the least time to become an activated carbon with the highest B.O. was RF. When blended with coal and BWM, it required more time to reach the same degree of burn-off. Whereas TC took even more time. For example, the time needed to reach a B.O. of 65 % was 400 < 820 < 1290 < 1320 < 1800 min for RF < RF/BWM < TC < RF/Coal < TC/Coal, respectively. This order reflects the reactivities of the different chars. The chars from RF and TC are composed of a mixture of carbonized elastomers and polymers together with the carbon black used in the preparation of the tyres. In the case of RF the polymer with the highest char yield is polyethylene terephthalate which hass an isotropic structure [39]. Disordered carbon reacts more quickly than well ordered, more graphitic carbon [38, 40]. Blends with coal were the slowest samples because coal required more time to be activated, since it is a less reactive material. To establish the degree of reactivity it is also very important to consider the effect of the composition of the ash present in the chars. Some elements such as potassium, sodium, calcium, magnesium and iron can cause an increase in the reaction rate due to a catalytic effect [41].

The elemental composition and ash contents of the activated carbons of each series vary as function of the burn-off, as shown Table 1. All of the samples have a high C content. However, these carbons also have high sulfur and ash contents which increase with the degree of burn-off. In general, a high ash content is a drawback in adsorption applications since the capacity of the adsorbent is considerably reduced [42]. The addition of coal and BWM to RF produced an increase in C and a decrease in the S and ash content of the ACs.

3.1. Textural characterization

Nitrogen adsorption isotherms of ACs prepared at 35 and 65 % B.O. were chosen in order to compare the differences between the materials prepared (Figure 2). The isotherms are of type IV, indicating that the ACs had mesopores. The main size range of the pores was 10-50 nm, as shown in Figure 3, although pores smaller than 2 nm and larger than 50 nm were also observed. In general, the amount of nitrogen adsorbed and the porosity were higher in the case of 65 % AC than 35 % AC since CO_2 had gasified some of the carbon in

the material, giving rise to more porosity. All the isotherms except those of RF/BWM indicate that an increase in B.O. produces an increase in the N_2 adsorbed at low relative pressure which is reflected in a widening of the microporosity and an increase in the mesopore volume. In the chars with BWM an increase in the B.O. was accompained by an increase in the mesopore volume in the 10-50 nm range (Figure 3). The greatest increase in micropore volume with the increase in B.O. occurred in the ACs containing coal. In the TC and TC/Coal there was also an increase in 10-50 nm and 2-3 nm mesopores (the latter to a lesser extent). TC also showed a larger increase in macropores than the other samples.

The evolution of S_{BET} with B.O. is shown in Figure 4, while the evolution of the total pore volume (V_t), the mesopore (V_{meso}) and micropore volume (V_{micro}) are presented in Figure 5.

It can be observed that the value of S_{BET} increased with the degree of B.O. until a maximum value was attained. A further increase in B.O. caused a decrease in the value of S_{BET} since the pores coalesced and became excessively large, damaging the porous texture. This occurred in all the samples except for the RF/BWM mixture which remained constant above 200 m^2/g.

The ACs from TC showed a higher S_{BET} for all degrees of burn-off than the ACs from RF. Moreover the maximum S_{BET} was obtained in the 55 and 80% B.O. range while in the case of RF a B.O. of 65% was needed to obtain a high surface area.

The evolution in pore volume with B.O. in the ACs from TC and RF (Figure 5a) shows that the gap in the total volumes was 0.20 cm^3/g at a burn-off smaller than 50%. When the B.O. increased, the difference in total volumes became smaller. The difference at 84% B.O. was 0.08 cm^3/g. This decrease in the difference in total volume must be due to the increase in the formation of micropores between 50 and 65%, and above 65% due to the more extensive formation of mesopores in RF as a consequence of activation.

The use of coal in the preparation of the ACs clearly increases the surface area, especially in the case of RF. The S_{BET} in the RF/Coal blend almost triples that of RF at 65 % B.O. This occurs even though the total pore volume is lower for all degrees of burn-off. The presence of coal produces a higher micropore volume with a consequent increase in S_{BET}.

3.2. Surface chemistry characterization

Surface functional groups present on the surface of activated carbon mainly affect their hydrophobic / hydrophilic and acidic / basic character. Consequently many of their applications will be conditioned by their chemical characteristics [42].

The characterization of the surface chemistry of ACs is not an easy task to perform and it is common to use two or more techniques that provide complementary information. The ACs obtained with 65 % B.O. were chosen for this study since they present the most developed textural characteristics.

The wavenumbers associated to signals in the FTIR spectra from chemical functional groups of interest are listed in Table 2. The spectra corresponding to wavenumbers in the range of 3500-2500 cm^{-1} and 2000-900 cm^{-1} are shown in Figure 6. The range between 3136-2997 cm^{-1} is associated to aromatic C-H stretching, whereas the range between 2997 and 2765 cm^{-1} is assigned to aliphatic C-H stretching. The 1693-1538 cm^{-1} range corresponds to the C=O and C=C stretching modes. Taking into account that oxygen-containing groups are the most common groups on carbon surfaces, special attention was paid to the C=O bond [43,44].

All the samples showed the same absorption bands at the same wavenumbers, indicating that the functional groups present were very similar. These ACs contained a variety of aromatic compounds, aliphatic compounds, and oxygenated functional groups, such as hydroxyl, carboxyl or carbonyl groups.

Curve-fitting of the peaks in the 1500-1800 cm^{-1} region provided integrated areas of the oxygenated and aromatic carbon groups, as in the case of TC (Figure 7). In order to make a correct interpretation of the spectra it is important to bear in mind that each functional group gives rise to bands at different wavenumbers The FTIR spectra of activated carbons indicate the presence of surface groups such as lactones, reflected in the bands in the ranges of 1160-1370 cm^{-1} and 1675-1790 cm^{-1}; quinones reflected in the C=O band between 1550 and 1680 cm^{-1} and carboxylic acids with bands in the ranges of 1120-1200, 1665-1760 and 2500-3300 cm^{-1} [43,44].

Wide-scan spectra in the binding energy range of approximately 0-1000 eV were obtained to identify the elements present on the AC surfaces and to perform a quantitative analysis (Figure 8). The most important elements in the wide scan spectra were oxygen (O), nitrogen (N), carbon (C), sulphur (S) and silicon (Si). Table 3 shows the peak center, normal area which is the peak area normalized taking into account the sensitivity factor of each element (C(1s):1.00, O(1s):2.85, N (1s): 1.77, S(2p):1.74 and Si (2p): 0.84) and percentage of each element for all the ACs at 65% B.O.

Of these elements, C was the most abundant (values from 83.3 wt.% for TC to 90.3 wt.% for RF/Coal). The percentage of carbon was higher in samples prepared with RF while the oxygen in TC and TC/Coal was even more abundant than in RF and RF/coal. The amount of nitrogen on the surface was negligible in all the samples. The percentage of silicon on the surface is related to the amount of ash which was higher in TC and the TC/Coal mixture.

Surface composition data obtained from the quantitative analysis of the peaks have been included in Table 4 together with the elemental composition of the bulk recalculated as atomic percentages. To be able to compare the two techniques the bulk composition was recalculated in an ash- and hydrogen-free basis (Table 4).

Carbon and sulphur contents in the bulk for all the samples and surfaces were very similar. The almost equivalent S contents suggest that sulphur must have been evenly distributed throughout the bulk of the material and on the external surfaces of the carbons because S was added uniformly to the tyres during the tyre manufacturing process. The greatest differences correspond to nitrogen and oxygen. While the nitrogen atomic content decreases on the surface, the oxygen content is significantly higher on the surface than in the bulk of the material. This is because oxygen reacted with carbon surface to form oxygenated functional groups, as a result of which the oxygen content on the surface increased.

Figure 9 and 10 show XPS spectra corresponding to C(1s) and O (1s) for TC and RF, and for the ACs prepared from blends TC/Coal, RF/Coal and RF/BWM, respectively. To

analyse the surface characteristics in more detail, the carbon and oxygen spectra were deconvoluted using Gaussian-Lorentzian peaks.

The broad carbon peaks corresponding to binding energies at approximately 282-298 eV can be attributed to carbon-based surface functional groups with various binding energies (BE).

When the C(1s) peak of the samples was deconvoluted, four peaks emerged. The peaks corresponding to Cgraphitic (BE = 284.4-284.5 eV), C-O in the hydroxyl bond (BE = 285.7 - 285.8 eV) and C=O in the carbonyl/quinone bond (BE = 287.0 - 287.4 eV) appeared in all samples [45-51]. The TC, RF and RF / BWM samples also showed a peak at BE = 289.4 - 289.7 eV corresponding to the carboxyl bond (O- C = O) [45, 52, 53]; while the mixtures with coal had carbonates (BE = 290.4 - 290.6 eV) [47, 50, 51]. The peak corresponding to the graphitic carbon shows the greatest intensity, as can be seen in Figures 9 and 10, and quantitatively, as a percentage, in Table 5 (46% to 63% of the detected carbon). This suggests that the surface chemistry of the activated carbon was not well developed. From the results it can also be seen that the peak of the hydroxyl bond was larger in the case of the TC sample (38%), because this bond was formed mainly during the pyrolysis of the tyre. Samples containing carbon showed a similar surface chemistry due to its extensive influence. All of these samples had the same amount of carbonyl and hydroxyl groups on their surface in addition to carbonates (8-10%).

The high-resolution spectra of C(1s) were very similar. Deconvolution yielded similar results considering that 46 to 63% of the area under the curve corresponded to graphitic carbon, whereas the carbon was as high as 85.5 - 91.9 % on the surface. Oxygen ranged from 11.8% for TC to 6.6% for RF on the surface, so that the intensity of this element was not as high as the case of the C(1s).

Deconvolution was also performed to study the high-resolution O(1s) spectrum of the samples. The RF, RF/Coal and RF/BWM samples had C=O bonds (BE = 530.7-531.7 eV) [45, 46, 51, 52, 54]. The peak corresponding to the C-O bonds in alcohols, ethers and peroxides (BE = 532.3 - 532.7 eV) [51, 52, 54] and the C-O bonds in peroxacids,

peroxyesters together with loading effects (BE = 534.6-535.0 eV) [54] appeared only in the RF and RF/BWM samples. C-O bonds from acids, esters and hydroperoxides were present on the surfaces of all the samples (BE = 533.1 - 533.8 eV) [45, 47, 51, 54]. On the other hand, the TC, TC/Coal and RF/Coal samples had occluded water, oxygen, CO_2 and CO (BE ~ 537 eV) [46, 55]. Because the measurements were performed under high vacuum conditions, only strongly adsorbed water, oxygen, CO_2 and CO were retained on the carbon surface. The high value of this peak in the spectrum corresponding to the TC, TC/Coal and RF/Coal samples indicates that these samples had many adsorption sites for water and/or gases such as oxygen, CO_2 and CO .

The presence of adsorbed gases would explain the large amount of oxygen that these materials had on their surface compared to their bulk, whereas RF and RF/BWM had a larger amount of oxygen in their bulk.

The results obtained by FTIR and XPS lead to the same conclusions for oxygenated surface groups. Both techniques indicate the presence of a C=O bond in the carbonyl/quinone group and a carboxyl bond in the carboxylic acids. A lactone bond was also observed in the XPS O1s of all the samples (Figure 9 and 10).

Conclusions

Activated carbons obtained from tyre wastes RF and TC, had S_{BET} in the range of 390 and 475 m^2/g with a pore size mainly in the mesopore range. However, their blends with coal give rise to an increase in their surface area to values similar to those of S_{BET} in commercial activated carbons (1125 and 840 m^2/g) due to an increase in their microporosity. Their drawback is that they are less reactive and therefore, they require more time for activation.

From the activation curves it can be seen that RF char is the most reactive material. The following order of reactivity was obtained RF>RF/BWM>TC>RF/Coal>TC/Coal. Nevertheless, the TC activated carbons prepared a had higher surface area at all degrees of burn-off and their maximum S_{BET} was obtained at a lower B.O. than in the case of RF.

The oxygenated functional groups present on the surface of the ACs were quinones, lactones and carboxylic acids.

Ackowledgements

The research leading to these results has received funding from the Spanish MICINN project reference CTM2009-10227. BA thanks the Government of the Principado de Asturias for the award of a pre-doctoral grant with funds from PCTI-Asturias.

References

[1] G. Newcombe, J. Morrison, C. Hepplewhite, Simultaneous adsorption of MIB and NOM onto activated carbon. I. Characterisation of the system and NOM adsorption, Carbon 40, (2002) 2135-2146.

[2] M.S. Dandekar, G. Arabale, K. Vijayamohanan, Preparation and characterization of composite electrodes of coconut-shell-based activated carbon and hydrous ruthenium oxide for supercapacitors, Journal of Power Sources, 141 (2005) 198-203.

[3] P. Chingombe, B. Saha, R.J. Wakeman, Surface modification and characterisation of a coal-based activated carbon, Carbon 43 (2005) 3132-3143.

[4] S. Ismadji, S.K. Bhatia, Characterization of activated carbons using liquid phase adsorption, Carbon 39 (2001) 1237-1250.

[5] J. Guo, A.C. Lua, Textural and chemical characterisations of activated carbon prepared from oil-palm stone with H_2SO_4 and KOH impregnation, Microporous and Mesoporous Materials 32 (1999) 111-117.

[6] M.I. Kandah, R. Shawabkeh, M.A. Al-Zboon, Synthesis and characterization of activated carbon from asphalt, Applied Surface Science 253 (2006) 821-826.

[7] I. Ozdemir, M. Şahin, R. Orhan, M. Erdem, Preparation and characterization of activated carbon from grape stalk by zinc chloride activation, Fuel Processing Technology 125 (2014) 200–206.

[8] A. Heidari, H. Younesi, A. Rashidi, A.A. Ghoreyshi, Evaluation of CO_2 adsorption with eucalyptus wood based activated carbon modified by ammonia solution through heat treatment, Chemical Engineering Journal 254 (2014) 503–513.

[9] M.C. Ncibi, R. Ranguin, M.J. Pintor , V. Jeanne-Rose , M. Sillanpää, S. Gaspard, Preparation and characterization of chemically activated carbons derived from Mediterranean Posidonia oceanica (L.) fibres, Journal of Analytical and Applied Pyrolysis 109 (2014) 205–214.

[10] A. Barroso-Bogeat, M. Alexandre-Franco, C. Fernández-González, V. Gómez-Serrano, Preparation of activated carbon-metal oxide hybrid catalysts: textural characterization, Fuel Processing Technology 126 (2014) 95–103.

[11] Z. Chen, K. Li, L. Pu, The performance of phosphorus (P)-doped activated carbon as a catalyst in air-cathode microbial fuel cells. Bioresource Technology 170 (2014) 379–384.

[12] K. Xia, J. Hu, J. Jiang, Enhanced room-temperature hydrogen storage in super-activated carbons: The role of porosity development by activation, Applied Surface Science 315 (2014) 261–267.

[13] H. Jin, X. Wang, Z. Gu, G. Anderson, K. Muthukumarappan, Distillers dried grains with soluble (DDGS) bio-char based activated carbon for supercapacitors with organic electrolyte tetraethylammonium tetrafluoroborate, Journal of Environmental Chemical Engineering 2 (2014) 1404–1409.

[14] D. Angin, Utilization of activated carbon produced from fruit juice industry solid waste for the adsorption of Yellow 18 from aqueous solutions, Bioresource Technology 168 (2014) 259-266.

[15] S. Hassan, L. Duclaux, J.-M. Lévêque, L. Reinert, A. Farooq, T. Yasin, Effect of cation type, alkyl chain length, adsorbate size on adsorption kinetics and isotherms of bromide ionic liquids from aqueous solutions onto microporous fabric and granulated activated carbons, Journal of Environmental Management, 144 (2014) 108-117.

[16] F. Zietzschmann, E. Worch, J. Altmann, A. S. Ruhl, A. Sperlich, F. Meinel, M. Jekel, Impact of EfOM size on competition in activated carbon adsorption of organic micro-pollutants from treated wastewater, Water Research 65 (2014) 297-306.

[17] B. Meryemoglu, S. Irmak, A. Hasanoglu, O. Erbatur, B. Kaya, Influence of particle size of support on reforming activity and selectivity of activated carbon supported platinum catalyst in APR, Fuel 134 (2014) 354-357.

[18] A. Mavrogiorgou, M. Papastergiou, Y. Deligiannakis, M. Louloudi, Activated carbon functionalized with Mn(II) Schiff base complexes as efficient alkene oxidation catalysts: Solid support matters, Journal of Molecular Catalysis A: Chemical 393 (2014) 8-17.

[19] G. Zhang, A. Su, Y. Du, J. Qu, Y. Xu, Catalytic performance of activated carbon supported cobalt catalyst for CO2 reforming of CH4, Journal of Colloid and Interface Science 433 (2014) 149-155.

[20] M.C. Tellez-Juárez, V. Fierro, W. Zhao, N. Fernández-Huerta, M.T. Izquierdo, E. Reguera, A. Celzard, Hydrogen storage in activated carbons produced from coals of different ranks: Effect of oxygen content, International Journal of Hydrogen Energy 39 (2014) 4996-5002.

[21] A. L. Cazetta, A. M.M. Vargas, E. M. Nogami, M. H. Kunita, M. R. Guilherme, A.C. Martins, T. L. Silva, J. C.G. Moraes, V. C. Almeida, NaOH-activated carbon of high surface area produced from coconut shell: Kinetics and equilibrium studies from the methylene blue adsorption, Chemical Engineering Journal 174 (2011) 117-125.

[22] M. Ghaedi, H. Mazaheri, S. Khodadoust, S. Hajati, M.K. Purkait, Application of central composite design for simultaneous removal of methylene blue and Pb2+ ions by walnut wood activated carbon, Spectrochimica Acta Part A: Molecular and Biomolecular Spectroscopy 135 (2015) 479-490.

[23] C. Namasivayam, D. Kavitha, Removal of Congo Red from water by adsorption onto activated carbon prepared from coir pitch, an agricultural solid waste. Dyes Pigments 54 (2002) 47 - 58.

[24] C. Namasivayam, N. Muniasamy, K. Gayatri, M. Rani, K. Ranganathan, Removal of dyes from aqueous solutions by cellulosic waste orange peel, Bioresour. Technol. 57 (1996) 37- 43.

[25] P. K. Malik, Use of activated carbons prepared from sawdust and rice-husk for adsorption of acid dyes: a case study of acid yellow 36, Dyes Pigments 56 (2003) 239 - 249.

[26] B. Acevedo, C. Barriocanal, R. Álvarez, Pyrolysis of blends of coal and tyre wastes in a fixed bed reactor and a rotary oven, Fuel 113 (2013) 817-825.

[27] T. Amari, N.J. Themelis, I.K. Wernick, Resource recovery from used rubber tires, Resources Policy 25 (1999) 179 - 188.

[28] M. Kyari, A. Cunliffe, V. Williams, Characterization of oils, gases and char in relation to the pyrolysis of different brands of scrap automotive tires, Energy Fuels 19 (2005) 1165 – 1173.

[29] R. Murillo, E. Aylón, M.V. Navarro, M.S. Callén, A. Aranda, A.M. Mastral, The application of thermal processes to valorise waste tyre, Fuel Process. Technol. 87 (2006)143 - 147.

[30] A.M. Fernández, C. Barriocanal, R. Alvarez, Pyrolysis of a waste from the grinding of scrap tyres, J. Hazard. Mater. 203– 204 (2012) 236 - 243.

[31] S. ÖnenÇ, M. Brebu, C. Vasile, J. Yanik, Copyrolysis of scrap tires with oily wastes, J Anal. Appl. Pyrolysis 94 (2012) 184 - 189.

[32] N. Antoniou, A. Zabaniotou, Features of an efficient and environmentally attractive used tyres pyrolysis with energy and material recovery, Renew. Sust. Energ. Rev. 20 (2013) 539 - 558.

[33] A.M. Mastral, R. Murillo, M.J. Perez-Surio, M.S. Callén, Coal hydrocoprocessing with tires and tire components, Energy Fuels 10 (1996) 941 - 947.

[34] B. Acevedo, C. Barriocanal, Fuel-oils from co-pyrolysis of scrap tyres with coal and a bituminous waste. Influence of oven configuration, Fuel 125 (2014) 155-163.

[35] A.M. Mastral, S. Callén, T. García, M.V. Navarro, Aromatization of oils from coal-tyre cothermolysis II. PAH content study as a function of the process variables, Fuel Process. Technol. 68 (2000) 45 - 55.

[36] M. Callén, V. Hall, A.M. Mastral, T. García, A. Ross, K.D. Bartle, PAH presence in oils and tars from coal-tyre coprocessing, Fuel Process. Technol. 62 (2000) 53 - 63.

[37] S.J. Gregg, K.S.W Sing, Adsorption, Surface Area and Porosity, Academic Press, London, 1997.

[38] F. Rodríguez-Reinoso, A.C. Pastor, H. Marsh, M.A. Martínez, Preparation of activated carbon cloths from viscous rayon. Part II: physical activation processes, Carbon 38 (2000) 379-395

[39] C. Barriocanal, M.A. Diez, R. Alvarez, PET recycling for the modification of precursors in carbon materials manufacture, J. Anal. Appl. Pyrolysis 73 (2005) 45–51.

[40] H. Marsh, K. Kuo, Kinetics and Catalyzing of formation of carbon gasification, in: H. Marsh (Ed.), Introduction to carbon science, Butterworths, London, 1989, pp. 107-152.

[41] D. Cazorla-Amorós, D. Ribes-Pérez, M.C. Román Martínez, A. Linares-Solano, Carbon 34 (1996) 869-878.

[42] T.J. Bandosz, Activated carbon surfaces in environmental remediation, Interface Science and Technology Vol.7, Elsevier, Amsterdam, 2006.

[43] J.L. Figueiredo, M.F.R. Pereira, M.M.A. Freitas, J.J.M. Órfao, Carbon 37 (1999) 1379-1389.

[44] B. Smith, Infrared spectral interpretation: a systematic approach, CRC Press, Boca Raton, 1998.

[45] H.-Y. Lin, W.-C. Chen, C.-S. Yuan, C.-H. Hung, Surface functional characteristics (C,O,S) of waste tire-derived carbon black before and after steam activation, J. Air and Waste Manage. Assoc. 58 (2008) 78-84.

[46] G. de la Puente, J.J. Pis, J.A. Menéndez, P. Grange, Thermal stability of oxygenated functions in activated carbons, J.Anal.Apply.Pyro 43 (1997) 125-138.

[47] J.P. Chen, S. Wu, Acid/Base- treated activated carbons: characterization of functional groups and metal adsorptive properties, Langmuir 20 (2004) 2233-2242.

[48] J. Przepiorski, J. Karolczyk, K. Takeda, T. Tsumura, M. Toyoda, A. W. Morawski, Porous Carbon Obtained by Carbonization of PET Mixed with Basic Magnesium Carbonate: Pore Structure and Pore Creation Mechanism, Ind. Eng.Chem. Res. 48, (2009) 7110-7116.

[49] P. Fan, C. Lu, A study on functionalization of waste tire rubber powder through ozonization, J. Polym Envirom 19 (2011) 943-949.

[50] C. Moreno-Castilla, M.V. López-Ramón, F. Carrasco-Marín, Changes in surface chemistry of activated carbons by wet oxidation, Carbon 38 (2000) 1995-2001.

[51] E. Desimoni, G. I. Casella, A. Morone and A. M. Salvi, XPS Determination of Oxygen-containing Functional Groups on Carbon-fibre Surfaces and the Cleaning of These Surfaces, Surface and Interface Anal 15 (1990) 627-634.

[52] A. Quek , R. Balasubramanian, Preparation and characterization of low energy post-pyrolysis oxygenated tire char, Chem Eng J 170 (2011) 194-201.

[53] S. Biniak, G. Szymaski, J. Siedlewski, A. Swiatkowski, The characterization of activated carbons with oxygen and nitrogen surface groups, Carbon 35 (1997) 1799-1810.

[54] P. Solís-Fernandez, J.I. Paredes, S. Villar-Rodil, L. Guardia, M.J. Fernandez-Merino, G. Dobrik, L.P. Biró, A. Martinez-Alonso, J.M.D. Tascón, Global and local oxidation behaviour of reduced graphene oxide, J Phys. Chem C. 115 (2011) 7956-7966.

[55] U. Zielke, K.J. Hüttinger, W.P. Hoffman, Surface-oxidized carbon fibers: I. Surface structure and chemistry, Carbon 34 (1996) 983-998.

Table 1. Elemental analysis and ash content for various degrees of activation.

Sample	B.O.*	Cz (wt% db)	C (wt% db)	H (wt% db)	N (wt% db)	S (wt% db)	O (wt% db)
TC	33%	22.3	75.8	0.3	0.3	2.9	8.2
	47%	27.9	69.8	0.3	0.6	3.7	2.0
	70%	37.8	58.7	0.2	0.5	4.2	1.6
RF	36 %	10.4	82.6	0.4	0.4	2.6	5.7
	47%	14.9	80.8	0.5	0.6	2.9	3.8
	56%	16.9	80.4	0.5	0.5	2.7	3.6
	66%	19.7	78.6	0.2	0.5	3.30	2.0
TC/Coal	38%	15.5	79.7	0.6	1.3	1.7	3.6
	51%	17.2	78.3	0.5	1.3	1.9	3.0
	66%	23.1	73.2	0.2	1.1	2.3	0.6
RF/Coal	34%	13.0	82.1	0.5	1.7	1.3	3.0
	47%	17.5	78.5	0.5	1.6	1.8	3.4
	59%	15.3	81.9	0.4	1.6	1.7	0.6
	65%	19.7	78.1	0.4	1.2	2.3	--
RF/BWM	35%	5.0	86.0	0.6	1.9	2.0	3.2
	56%	15.4	81.0	0.5	1.6	2.6	3.4
	61%	12.3	82.3	0.5	1.5	2.8	2.6

*B.O.: burn-off expressed on an ash free basis.

Table 2. Band assignments for the FTIR spectra.

Wavenumber (cm^{-1})	Assignment
3300	-OH and –NH stretching
3136-2997	Aromatic compounds C-H stretching
2997-2765	Aliphatic compounds C-H stretching
1770-1650	C=O Oxygenated groups
1600	C=C Aromatic compounds - ring stretching
1455	Bending vibrations of C-H bonds in $-CH_2-$ and $-CH_3$ groups
1375	$-CH_3$ Symmetric bend

Table 3. Surface composition of ACs prepared at 65% B.O.

	Peak	Peak centre	Normal Area	Atomic percentage (%)
TC	O (1s)	534.0	3371.5	11.5
	N (1s)	398.0	92.3	0.3
	C (1s)	285.0	24339.7	83.0
	S (2p)	164.5	679.1	2.3
	Si (2p)	107.5	832.1	2.8
RF	O (1s)	533.0	1822.9	6.6
	N (1s)	398.0	98.0	0.4
	C (1s)	285.0	25044.9	90.1
	S (2p)	164.5	518.3	1.9
	Si (2p)	102.5	313.4	1.1
TC/Coal	O (1s)	538.0	2583.3	10.0
	N (1s)	400.0	29.9	0.1
	C (1s)	285.0	22121.6	85.4
	S (2p)	164.5	112.4	0.4
	Si (2p)	108.5	1042.1	4.0
RF/Coal	O (1s)	533	1662.0	6.7
	N (1s)	401.5	170.6	0.7
	C (1s)	285.0	22458.7	90.3
	S (2p)	164.5	139.6	0.6
	Si (2p)	105.5	433.3	1.7
RF/BWM	O (1s)	533.0	2161.1	10.0
	N (1s)	401.0	25.1	0.1
	C (1s)	285.0	18871.0	87.4
	S (2p)	164.5	266.3	1.2
	Si (2p)	103.0	262.1	1.2

Table 4. Bulk and surface composition of ACs prepared at 65% B.O.

		C (%at.)	N (%at.)	S (%at.)	O (%at.)
TC	bulk	94.8	0.7	2.5	1.9
	surface	85.5	0.3	2.4	11.8
RF	bulk	96.1	0.5	1.5	1.8
	surface	91.1	0.4	1.9	6.6
TC/Coal	bulk	97.0	1.3	1.1	0.6
	surface	89.0	0.1	0.5	10.4
RF/Coal	bulk	97.1	1.6	0.8	0.5
	surface	91.9	0.7	0.6	6.8
RF/BWM	bulk	95.0	1.5	1.2	2.3
	surface	88.5	0.1	1.2	10.1

Table 5. Surface functional components obtained from the deconvolution of C(1s) peaks.

Peak	Surface Functional Group	B.E (eV)	TC (%)	RF (%)	TC/Coal (%)	RF/Coal (%)	RF/BWM (%)
C1s_1	C-C	284.4 - 284.5	46	63	56	59	61
C1s_2	C-O	285.7 - 285.8	38	17	18	16	20
C1s_3	C=O	287.0 - 287.4	4	6	18	15	11
C1s_4	O-C=O	289.4 - 289.7	12	14	-	-	8
C1s_5	carbonates	290.4 - 290.6	-	-	8	10	-

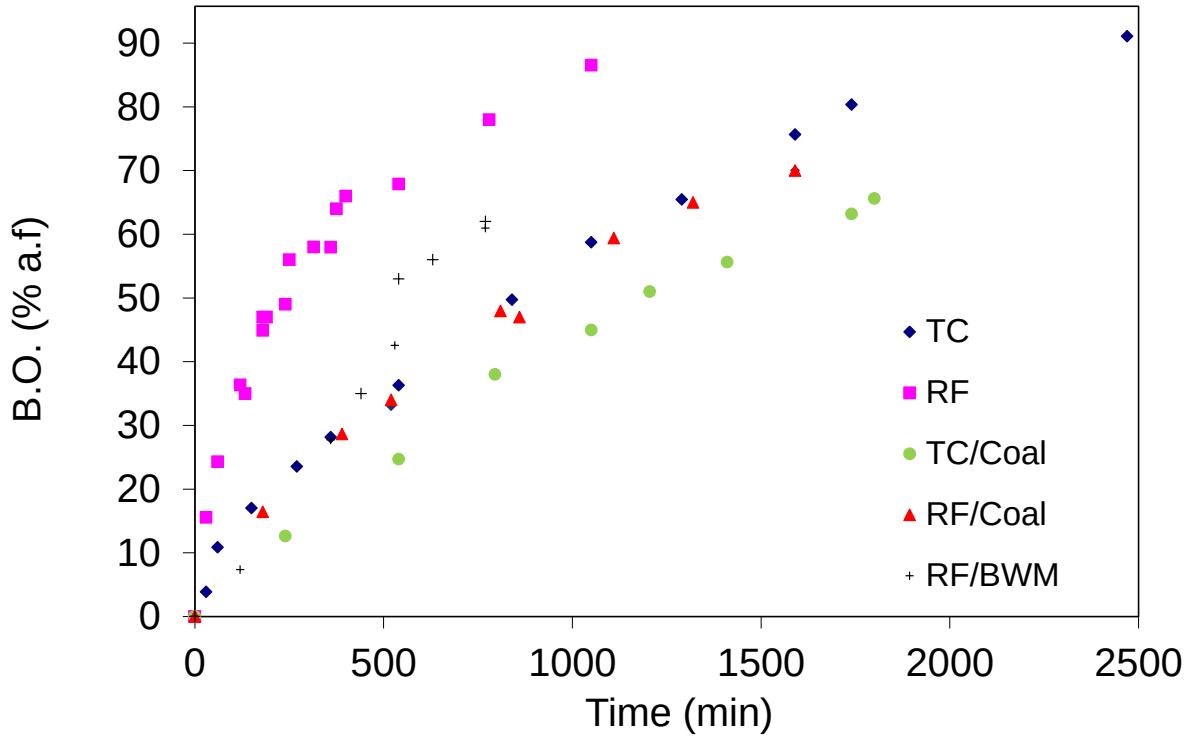

Figure 1. Variation of carbon burn-off (B.O.) with time.

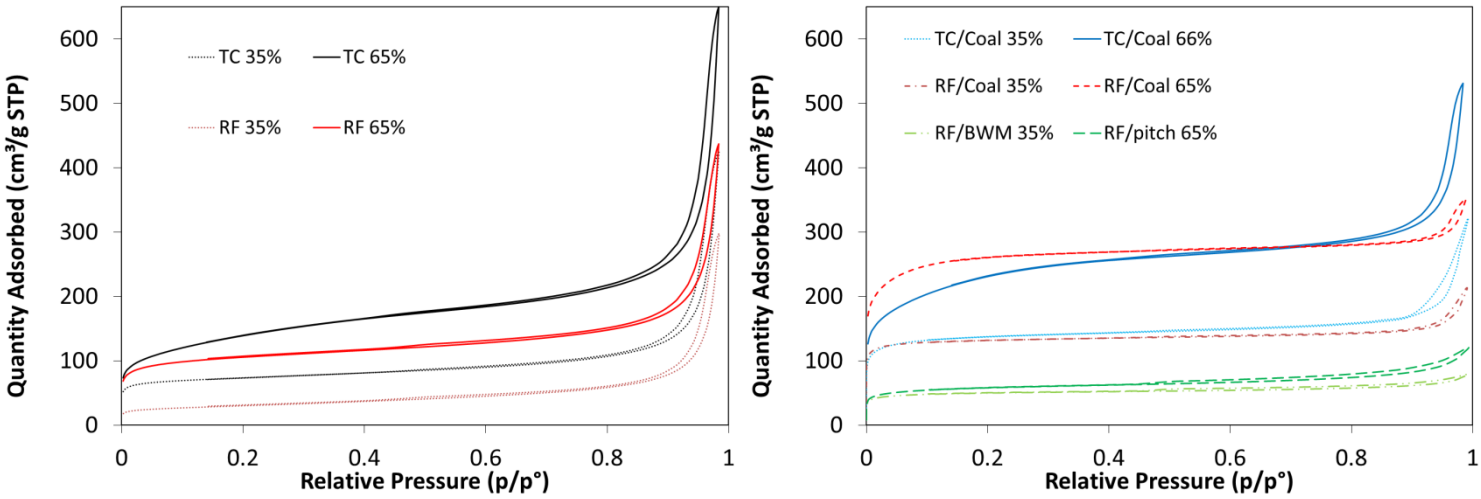

Figure 2. Adsorption isotherms of nitrogen at 77 K for ACs prepared at 35 % and 65 % B.O.

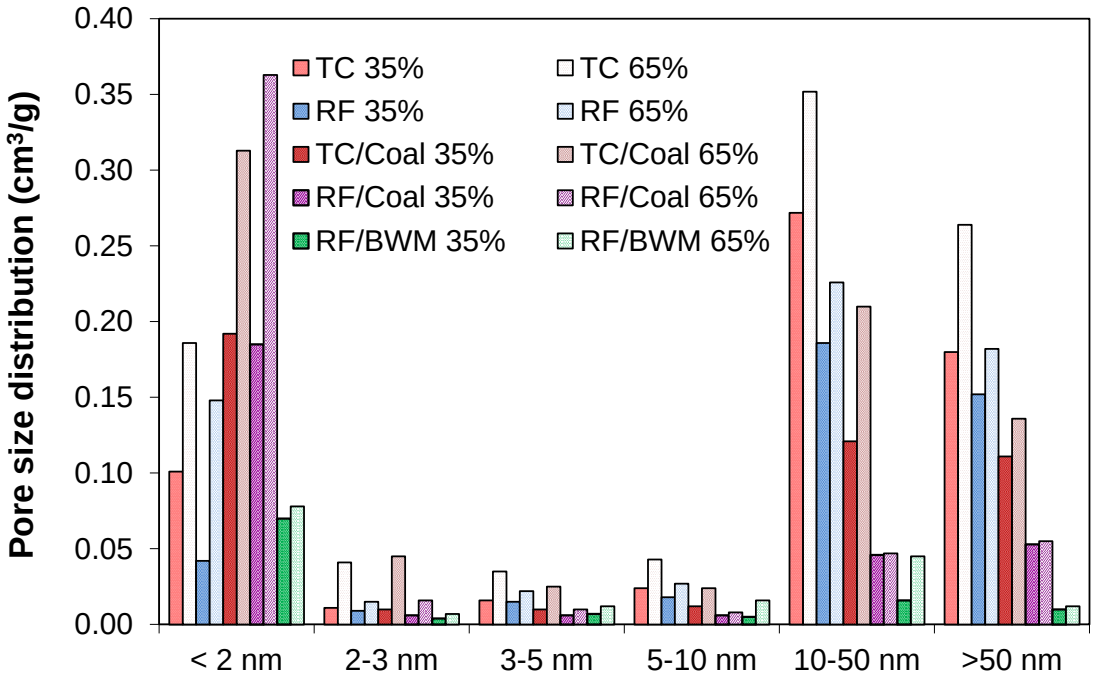

Figure 3. Pore size distribution by Kelvin for ACs prepared at 35% and 65% B.O.

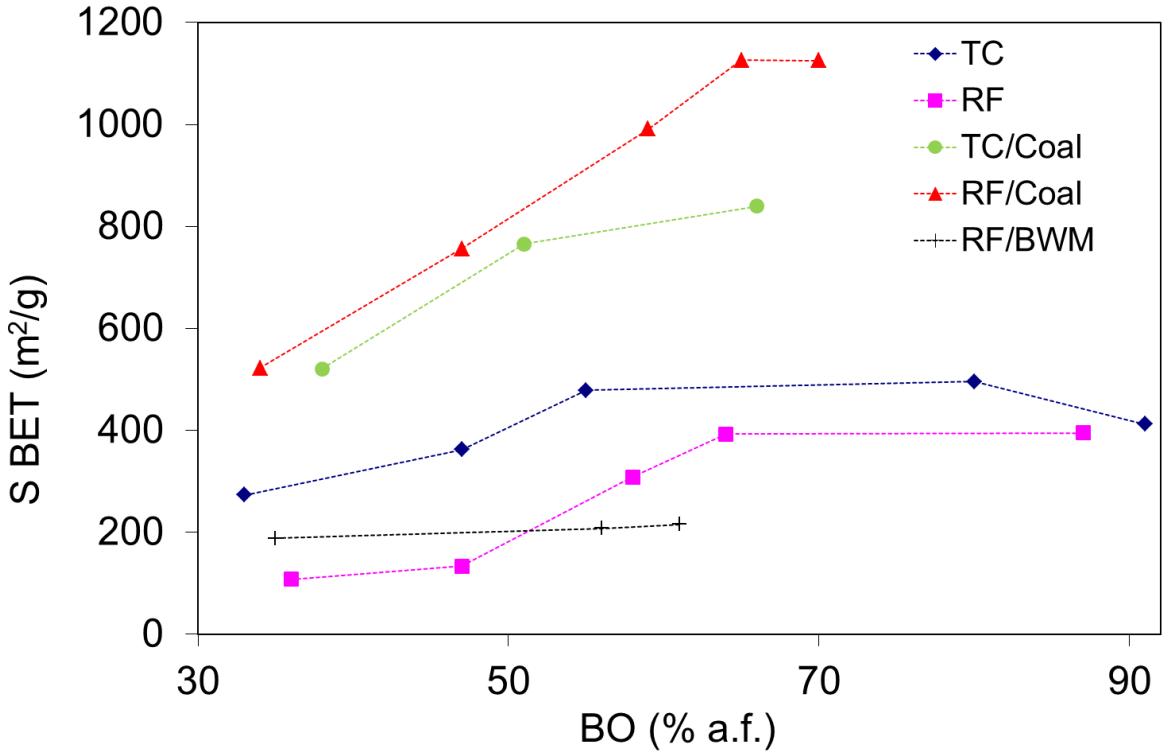

Figure 4. Variation of S_{BET} with B.O.

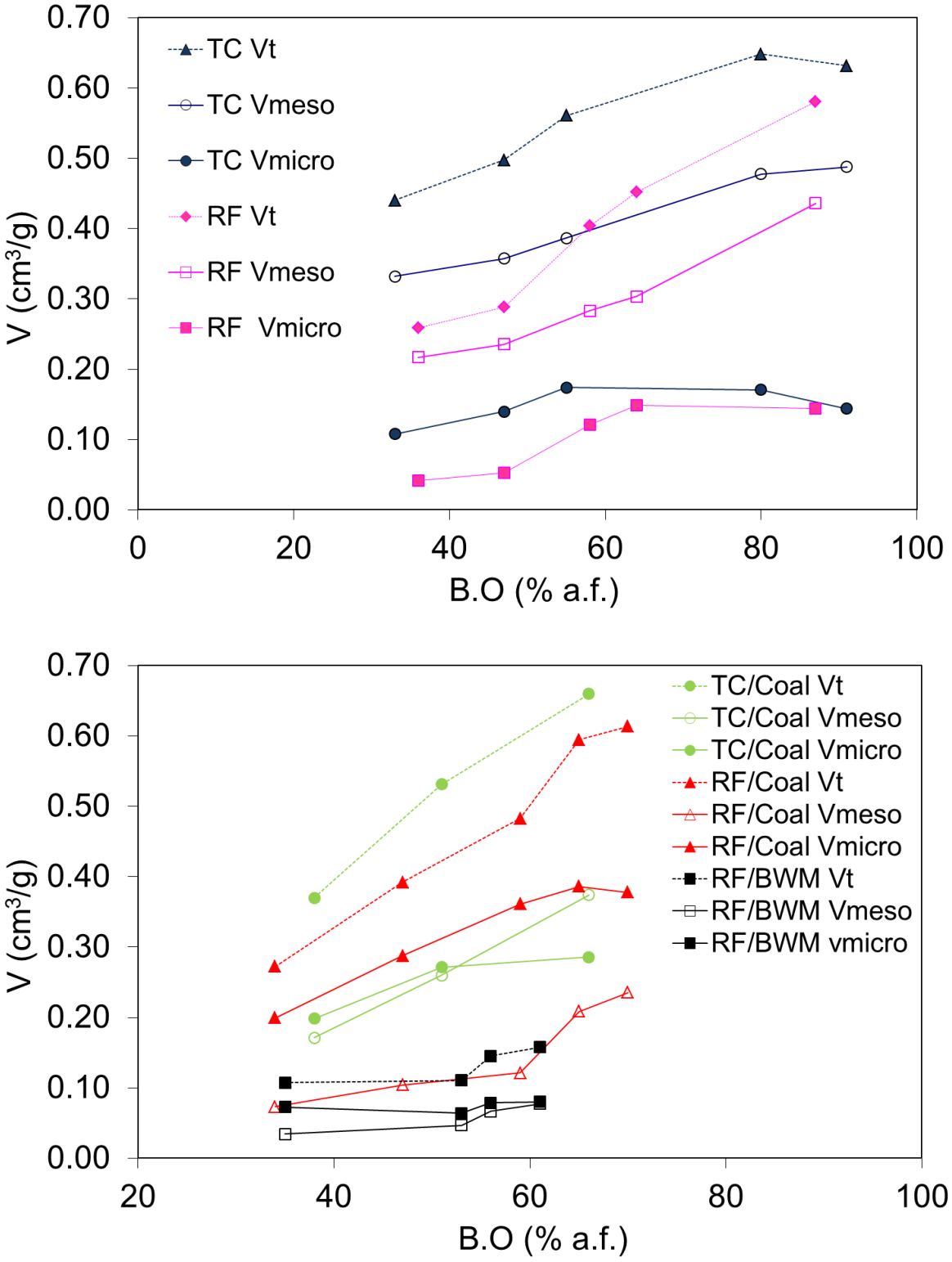

Figure 5. Variation of pore volume with B.O.

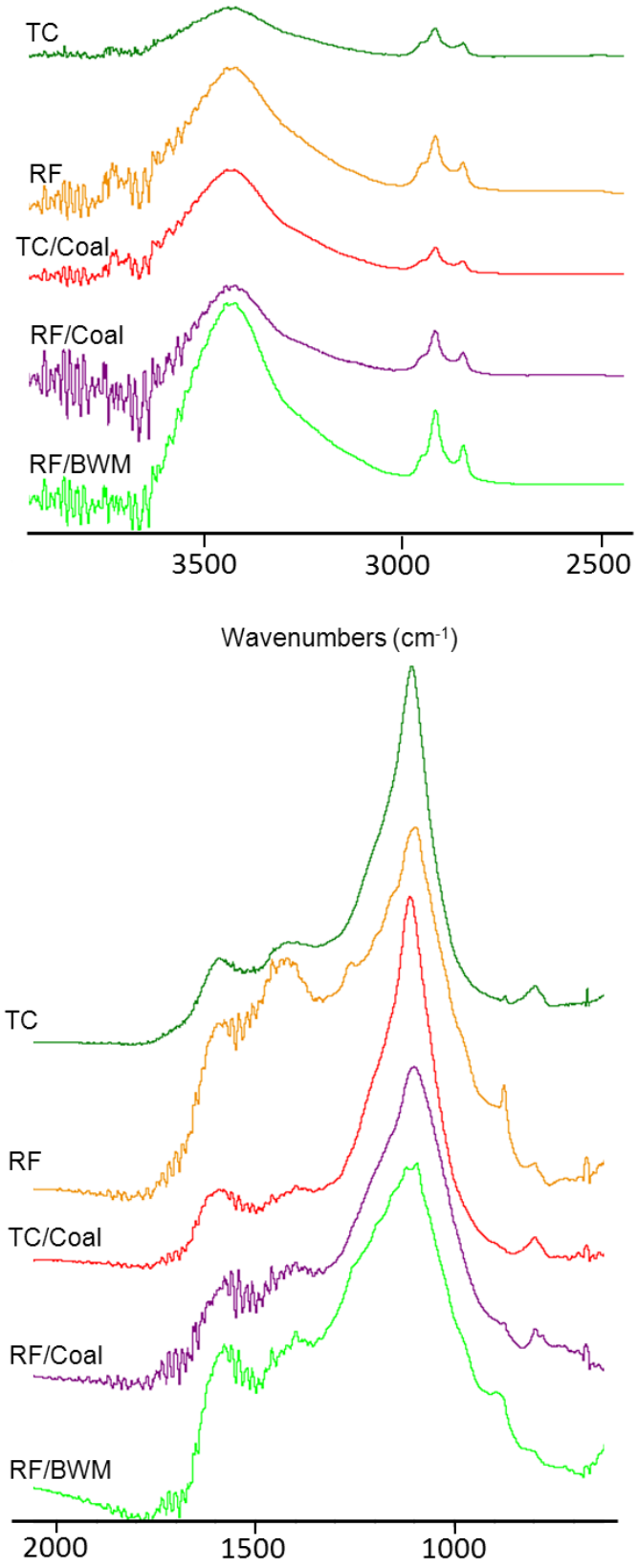

Figure 6. FTIR AC produced at 65 % B.O.

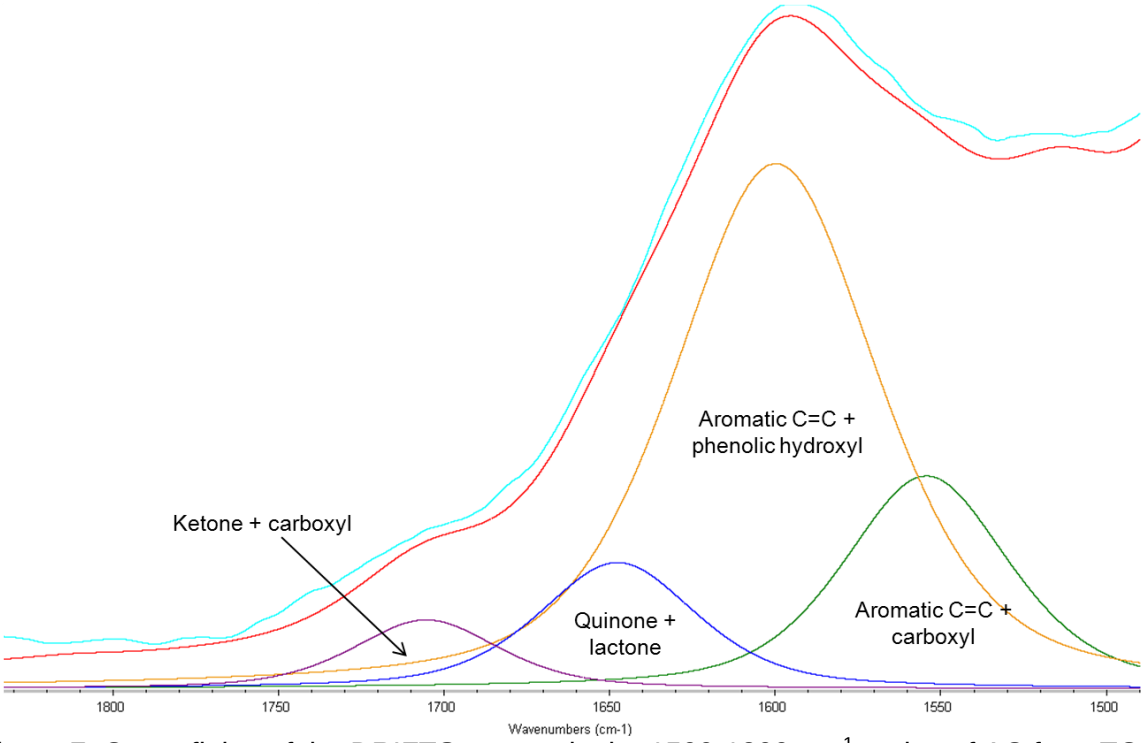

Figure 7. Curve-fitting of the DRIFTS spectra in the 1500-1800 cm^{-1} region of AC from TC at 65% B.O.

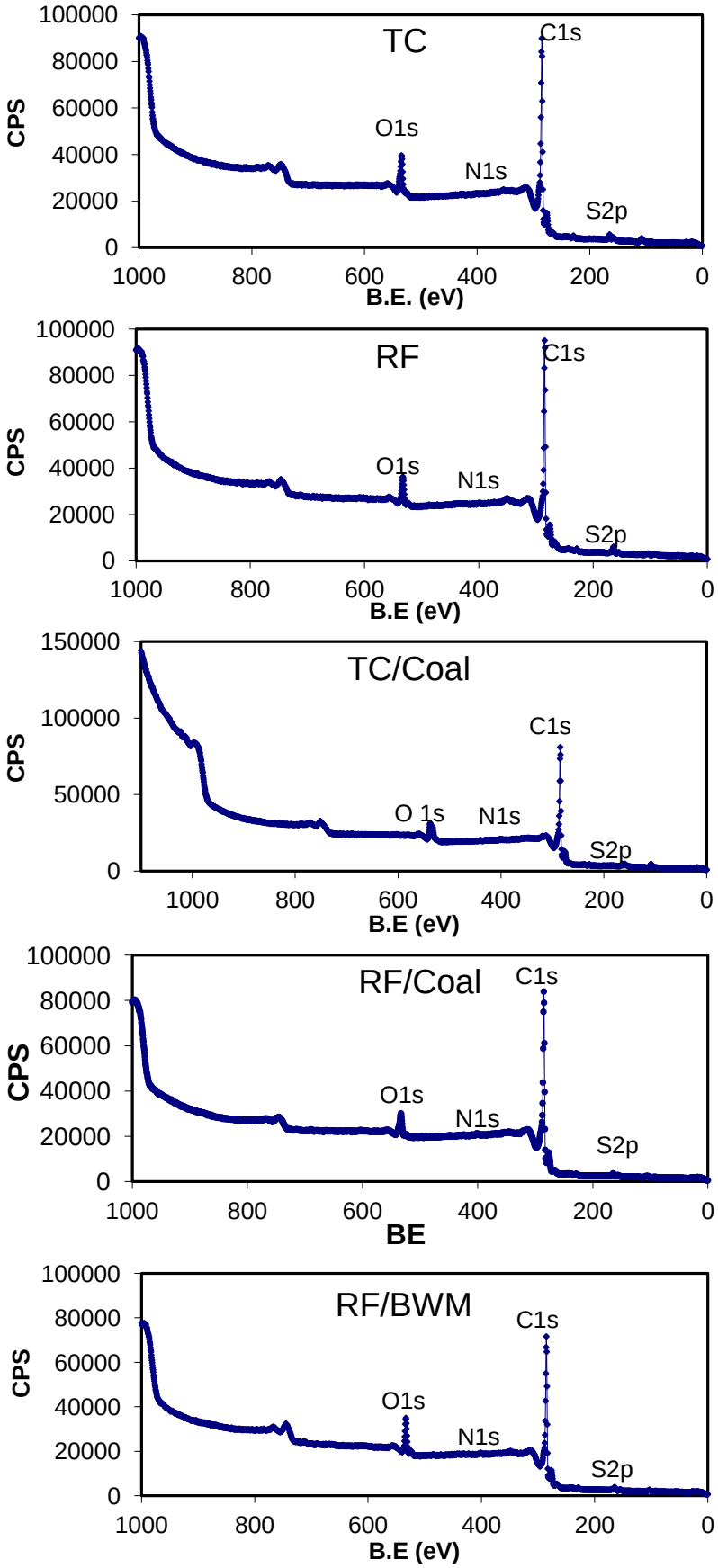

Figure 8. Wide scan spectra for AC TC,RF,TC/Coal, RF/Coal and RF/BWM.

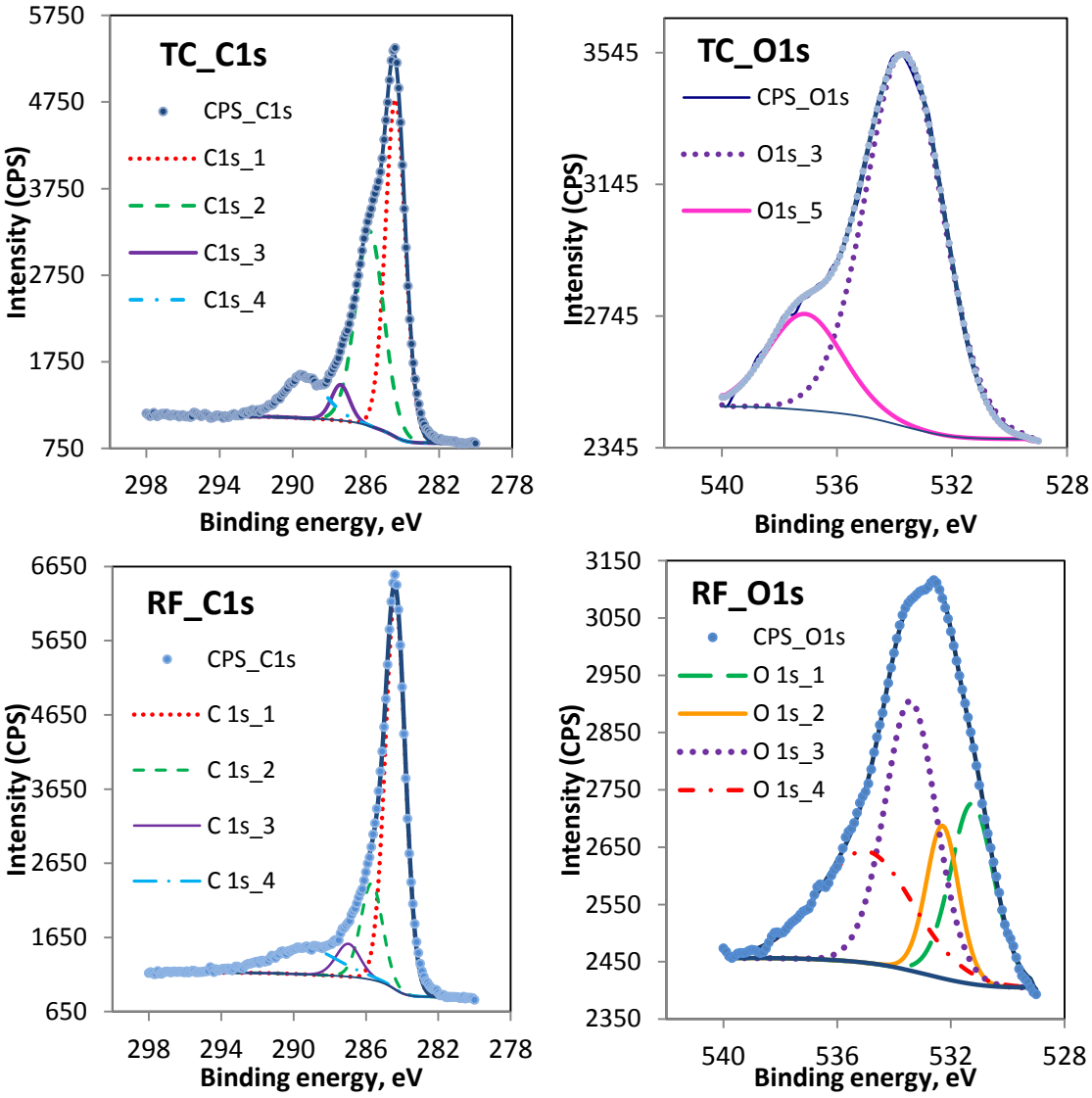

Figure 9. XPS spectra corresponding to C(1s) and O(1s) of activated carbons: TC and RF 65% B.O.

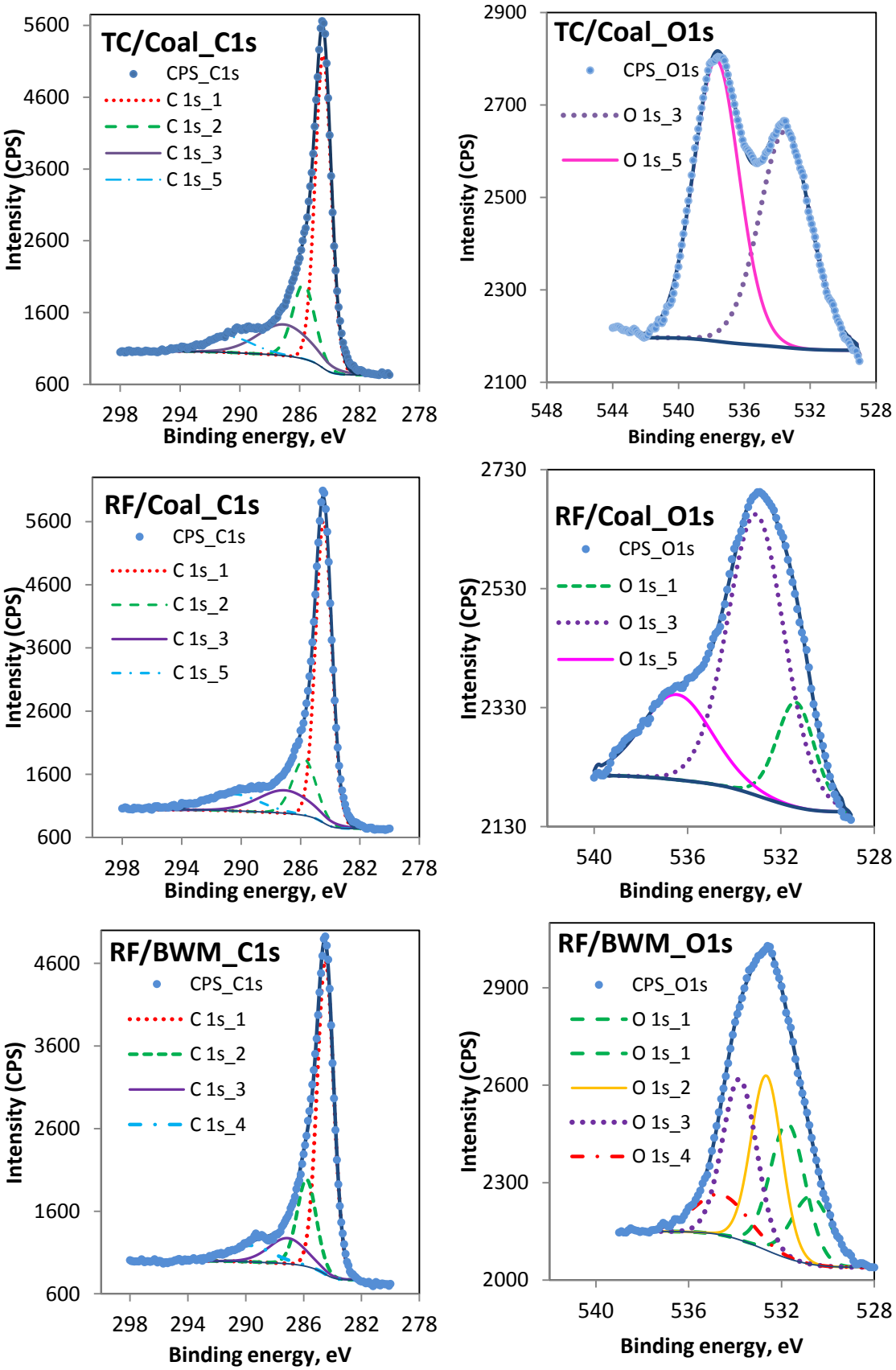

Figure 10. XPS spectra of C(1s) and O(1s) of TC/Coal, RF/Coal and RF/ BWM 65% a.f.